Renal Perfusional Cortex Volume for Arterial Input Function Measured by Semiautomatic Segmentation Technique Using MDCT Angiographic Data With 0.5-mm Collimation

Izumi Torimoto[1]
Shigeo Takebayashi[2]
Zenjiro Sekikawa[2]
Junichi Teranishi[3]
Keiji Uchida[4]
Tomio Inoue[1]

OBJECTIVE. The purpose of this study was to evaluate the usefulness of renal perfusional cortex volume for arterial input function.

MATERIALS AND METHODS. This retrospective study included 45 potential kidney donors—33 patients with aortic dissection and 12 patients with renovascular hypertension—who underwent both MDCT angiography with 0.5-mm collimation and renal ^{99m}Tc-diethylenetriamine pentaacetic acid (DTPA) scanning using the modified Gates method. Each perfusional cortex volume for the arterial input function and parenchymal volume was measured by semiautomatic segmentation using the region-growing technique. Linear regression analysis and correlation coefficients were used to assess the impact of the cortical volume, parenchymal volume, and renal scanning glomerular filtration rate (GFR) on estimated GFR (eGFR) using a modified Modification of Diet in Renal Disease (MDRD) equation.

RESULTS. The correlation coefficient was higher for the total renal DTPA GFR adjusted for body surface area, weight-adjusted perfusion cortex volume, and adjusted total parenchyma volume in rank ($r = 0.712$, 0.642, 0.510, respectively, $p < 0.0001$ for each). The coefficient of the right renal perfusional cortex volume percent with a mean value of 52.1% ± 10.1% was 0.826 ($p < 0.0001$) for the right renal DTPA GFR percent with a mean value of 51.0% ± 12.1% (range, 22.0–89.5%), although the value for the right renal parenchymal volume percent with a mean value of 49.5% ± 5.5% was 0.764 ($p < 0.0001$).

CONCLUSION. Weight-adjusted perfusional cortex volume for arterial input function can be measured clinically and may replace renal DTPA scanning using the modified Gates method.

Keywords: glomerular filtration rate, MDCT, renal scintigraphy, renal volume, segmentation algorithm

DOI:10.2214/AJR.14.12778

Received March 1, 2014; accepted after revision April 9, 2014.

[1]Department of Radiology, Yokohama City University Graduate School of Medicine, Yokohama, Japan.

[2]Department of Diagnostic Radiology, Yokohama City University Medical Center, 4-57, Urafune-cho, Minami-ku, Yokohama, 232-0024, Japan. Address correspondence to S. Takebayashi (take2922@yokohama-cu.ac.jp).

[3]Department of Urology, Yokohama City University Medical Center, Yokohama, Japan.

[4]Department of Cardiovascular Surgery, Yokohama City University Medical Center, Yokohama, Japan.

AJR 2015; 204:98–104

0361–803X/15/2041–98

Renal diethylenetriamine pentaacetic acid (DTPA) scanning performed with the modified Gates method without blood and urine collection is a commonly used technique to determine renal blood flow and split renal function. The technique provides notable information, such as quantitative unilateral renal function and pathophysiologic changes in the kidney in renovascular disease, hydronephrosis, and renal transplantation [1–3]. Renal volume is important for renal transplantation planning regarding decisions concerning the donor kidney site and for renovascular diseases regarding decisions concerning whether to perform an interventional procedure. Compared with complicated and time-consuming manual volumetric assessment as the plotting contour method, automatic or semiautomatic segmentation using various postprocessing techniques can greatly reduce the required time and increase the potential accuracy of measurement [4–6].

Several studies have investigated renal cortex segmentation on MDCT and MRI in donors because glomerular filtration rate (GFR) is the main functional parameter of the renal cortex [5, 7–9]. Yano et al. [9] reported that there was a positive coefficiency for renal cortical volume to recipient weight that was associated with diminished renal function at long-term follow-up after transplantation, but there have been no other studies showing that the renal cortex volume has a stronger correlation with renal function than renal parenchymal volume. Advances in MDCT, including 64-MDCT technology, allow faster acquisition of volumetric image data with superior *z*-axis resolution with thin collimation for CT angiography and quantitative perfusion analysis for kidney allograft dysfunction [10]. Volumetric data acquired with a thinner collimation is expected to provide more accurate volume measurement.

In this retrospective study, we measured the volume of the renal perfusional cortex for

TABLE 1: Demographics in 90 Subjects Who Underwent Both Renal Artery MDCT and Renal Diethylenetriamine Pentaacetic Acid Scanning

Demographic	Possible Living Kidney Donors (n = 45)	Patients With Aortic Dissection (n = 33)	Patients With Renovascular Hypertension (n = 12)	Total
Mean age ± SD (y)	57.6 ± 9.4	66.4 ± 9.0	63.2 ± 13.7	61.5 ± 10.1
Male/female	26/19	22/11	8/4	56/34
Mean weight ± SD (kg)	61.8 ± 8.1	66.0 ± 10.3	70.0 ± 5.9	64.4 ± 9.1
Mean BSA ± SD (m^2)	1.67 ± 0.13	1.70 ± 0.14	1.80 ± 0.12	1.70 ± 0.14
Mean serum creatinine ± SD (mg/dL)	0.79 ± 0.18	1.08 ± 0.37	1.00 ± 0.15	0.92 ± 0.29
Mean eGFR ± SD (mL/min/1.73 m^2)[a]	72.5 ± 13.5	54.8 ± 17.3	60.6 ± 14.1	64.5 ± 17.0

Note—BSA = body surface area, eGFR = estimated glomerular filtration rate.
[a]Calculated by the modified abbreviated Modification of Diet in Renal Disease equation for Japanese.

the arterial input function by semiautomatic MDCT segmentation using the region-growing method from MDCT angiographic data with 0.5-mm collimation. The volumetric data obtained by scanning with more than 80-MDCT can be expected to enable more accurate measurement of renal volume because it eliminates the problem of stair-step artifacts associated with helical and step-and-shoot scanning techniques. Next, we evaluated the usefulness of the cortical volume measurement in a quantitative prediction of unilateral renal function compared with renal parenchymal volume measurement and renal DTPA scanning in patients who underwent MDCT angiography.

Materials and Methods

Study Group

Approval for this retrospective study was obtained from our institutional review board. We confirmed that the patients in this study were given a comprehensive written statement of information about the clinical study, including information on MDCT and renal scanning. The clinical and radiologic database sets at our hospital were searched for 90 consecutive subjects in whom both renal DTPA scanning and MDCT abdominal angiography with 0.5-mm collimation were performed between January 2012 and October 2013. All subjects were of Japanese ethnicity. The population consisted of 45 possible living kidney donors between 35 and 77 years old, 33 patients with aortic dissection (type A, 12 cases; type B, 21 cases) between 44 and 86 years old, and 12 patients with renovascular hypertension (8, arteriosclerosis; 4, fibromuscular dysplasia) between 26 and 80 years old (Table 1). The interval period between MDCT angiography and renal scanning, when serum creatinine, height, and weight were measured, was within 1 week in all donors and patients. Estimates of kidney function were provided by estimated GFR (eGFR) using the modified Modification of Diet in Renal Disease (MDRD). For Japanese men, the MDRD equation is as follows: 194 × [serum creatinine (μmol/L)]–1.904 × [age]–0.287 mL/min/1.73 m2; for Japanese women, 194 × [serum creatinine (μmol/L)]–1.904 × [age]–0.287 × 0.739 mL/min/1.73 m2 [11].

Scanning With ^{99m}Tc-DTPA

Split GFR was measured with the modified Gates method [1] using a gamma camera (Millennium VG SPECT, GE Healthcare) after a bolus IV injection of 111 MBq of ^{99m}Tc-DTPA. Then, we obtained the total renal scanning GFR, renal scanning GFR for each kidney, and right renal scanning GFR percent, which is calculated as follows: (*right renal scanning GFR / total renal GFR*) × 100.

MDCT Volumetric Data Acquisition

The volumetric data with 0.5-mm thickness were acquired using a 160-MDCT unit (Aquilion Premium, Toshiba Medical Systems) after a 100-mL bolus of 300 mg I iopamidol was injected at a rate of 3 mL/s. For the evaluation of renal arteries, the data from above the kidneys to the pubic symphysis were acquired by 80-MDCT scanning (80 mm × 0.5-mm collimation, beam pitch of 0.813, rotation speed of 0.5 second, table speed of 32.5 mm per rotation, and voltage of 120 kVp), whereas for the evaluation of total aorta and renal arteries, the data from the neck to the pubic symphysis were acquired by 160-MDCT scanning (160 mm × 0.5-mm collimation, beam pitch of 0.870, rotation speed of 0.5 second, table speed of 139 mm per rotation, and voltage of 120 kVp). Bolus tracking was used in the aorta at the level of the celiac axis for the angiographic phase. Scanning of the abdomen was initiated 10 seconds after a threshold enhancement of 150 HU on 80-MDCT scanning, and that of both the thorax and abdomen was initiated 7 seconds after a threshold enhancement of 230 HU on 160-MDCT scanning. An adaptive iterative dose-reduction algorithm in 3D (AIDR-3D, Toshiba Medical Systems) was used for 20–30% reduction of radiation exposure. The reconstructed data were 0.5-mm thickness and 0.5-mm interval in both the angiographic and parenchymal phases.

Segmentation Technique

The postprocessing software that we used was a commercially available application, liver volume analyzer (Synapse Vincent 3D, Fujifilm Medical), which supports liver extraction, vessel analysis, liver segmentation, and volumetry. The software processing was retrospectively performed in a PACS (Synapse, version 3.1, Fujifilm Medical). In 96.7% (87) of the 90 subjects, a semiautomatic region-growing segmentation of the renal perfusional cortex and renal parenchyma were performed using MDCT volumetric data in the angiographic phase. In the remaining three patients with aortic dissection, however, the parenchymal phase was selected when the renal artery was connected to the aortic false lumen and was not enhanced on the angiographic phase but instead on the parenchymal phase.

The segmentation technique was performed in four steps. In step 1, a 3D-volume-rendering image of the liver was extracted automatically by the liver volume analyzer in which highlighted areas in the axial, sagittal, and coronal maximum-intensity-projection (MIP) images indicated the region information on the basis of the growing technique. Then, an interactive 3D cutting was performed to remove the liver. In step 2, a seed point was interactively selected in the renal cortex for segmentation of only the perfusional cortex or both the cortex and medulla for segmentation of the renal parenchyma via mouse clicking, and the resulting selection of neighboring pixels within the same region displayed similar attenuation (Fig. 1A). A few seed points were interactively selected in the target by mouse clicking. In step 3, manual editing was performed to remove the nontarget extracted parts, such as renal arterial branches, which have similar contrast enhancement as the renal cortex (Fig. 1B). This was also achieved by deletions of highlighted pixels in the MIP images. In step 4, the volume of the segmented cortex was measured automatically. Five to 10 minutes were required for these four steps to obtain a segmentation of renal perfusional cortex. Obtaining a segmentation of renal pa-

renchyma required 3–5 minutes when several seed points were selected in the medulla on the MIP image of a segmentation for the renal cortex (Fig. 1C).

Imaging Analysis

All of the users and reviewers for all of the postprocessing techniques were blinded to the subjects' histories and outcomes during independent segmentation technique performance. The findings of the renal artery on MDCT angiography were evaluated by a reviewer who was a radiologist with 10 years of abdominal imaging experience. In regard to contrast flow in the renal artery, the findings were divided into normal flow and possibly disturbed flow. Configurations of the artery were classified into normal artery, artery connected to a false lumen of the dissecting aorta, artery connected to a compressed true lumen of the dissecting aorta, and artery with stenosis. The segmentation technique was performed to measure each of the perfusion cortex volumes and parenchymal volumes by two users: User 1 was a radiologist with 20 years of abdominal imaging experience. User 2 was a technician with 3 years of experience in measurements using MDCT volumetric data. Furthermore, user 1 also repeated the segmentation after a 1-month interval to assess intraobserver variability.

Statistical Analysis

Statistical analyses were performed using Microsoft Excel add-on software, Xlstat (Addinsoft). Inter- and intraobserver agreements in the cortex volume and the parenchyma volume, measured by using semiautomatic region-growing segmentation, were tested with the Bland-Altman plot method to estimate 95% CIs for the bias and limits of agreement. Using the first dataset of user 1, Pearson or Spearman rank correlation coefficients were used to assess the correlation of each subject's total perfusional cortex volume, total parenchyma volume, and total renal scanning GFR compared with each factor of the demographics. Simple linear regression analyses were performed to assess the impact of each measurement adjusted for body habitus (weight and body surface area [BSA]) on the eGFR. The correlation was also calculated between the relative renal scanning GFR of the right kidney, expressed as a percentage (right DTPA GFR percent) and both the right perfusional cortex and parenchymal volume percent in all subjects. The absolute value of the correlation coefficient was interpreted as no relationship (< 0.2), weak relationship (0.2 to < 0.5), moderate relationship (0.5 to < 0.8), and strong relationship (0.8 to < 1) [12]. Values for $p < 0.05$ were considered statistically significant.

Results

The demographics of the 90 subjects are listed in Table 1. The mean age of the potential kidney donors was greater than pa-

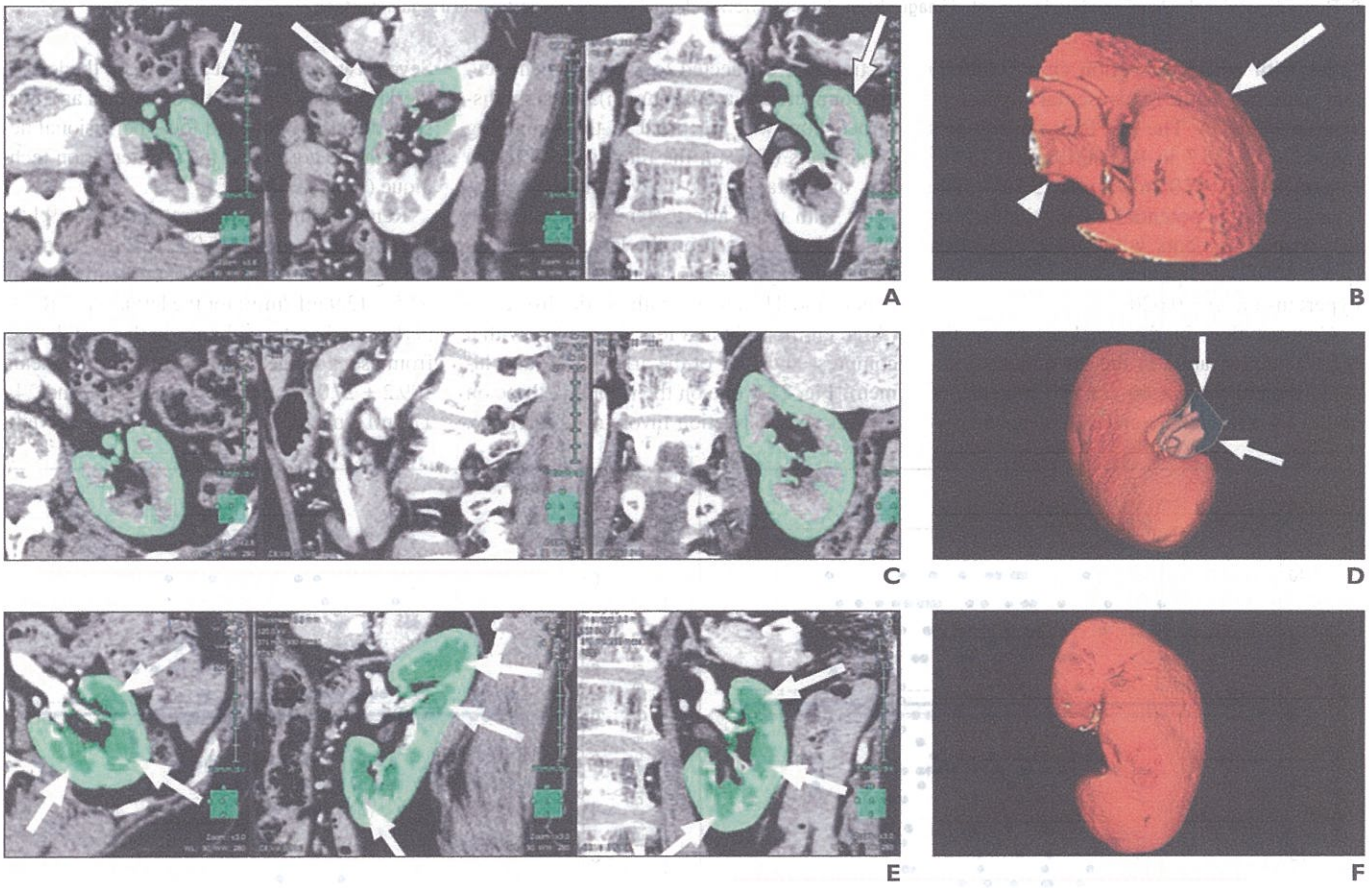

Fig. 1—54-year-old man who was possible living kidney donor.
A, Maximum-intensity-projection images show perfusional cortex (*arrows*) in left renal upper pole and renal vessels (*arrowhead*) at renal hilum segmented and displayed.
B, Highlighted cortex (*arrow*) and vessels (*arrowhead*) are shown on 3D volume-rendered image after seed point is interactively selected in renal cortex by mouse clicking.
C and **D,** Interactive cutting (*arrows*) is performed to remove vessels, shown on 3D maximum-intensity-projection images (**C**) and volume-rendered image (**D**) of extraction result. Several cuttings are required in complete removal of vessels.
E and **F,** Maximum-intensity-projection images (**E**) and volume-rendered image (**F**) show segmentation of left renal parenchyma (*arrows*) performed after adding highlights in medullas in extracted perfusion cortex.

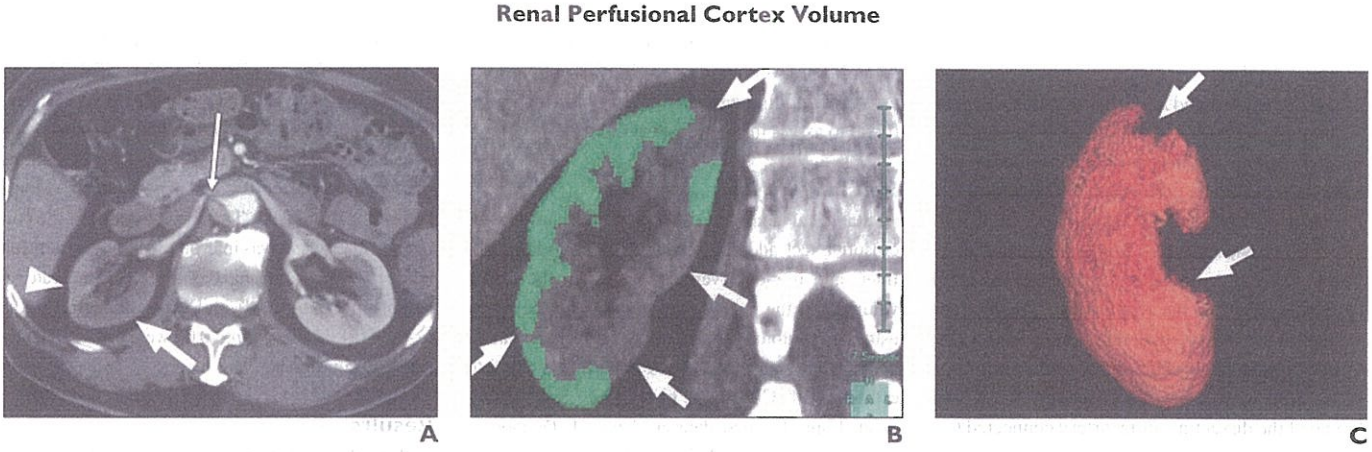

Fig. 2—72-year-old man with type B aortic dissection.
A, Axial MDCT image of right kidney shows compressed orifice (*thin arrow*) of right renal artery by false lumen and decreased perfusion cortex with predominance of posteromedial portion (*thick arrow*) compared with anterolateral portion (*arrowhead*).
B, Coronal maximum-intensity-projection image of right kidney after extraction of perfusion cortex area (*green*) shows nonperfusion areas (*arrows*).
C. Three-dimensional volume-rendered segmented image shows defects (*arrows*) of renal perfusional cortex and irregular surface.

tients with aortic dissection (p = 0.00011) and patients with renovascular hypertension (p = 0.020). The eGFR in the subjects ranged from 25.7 to 93.6 mL/min/1.73 m^2 (mean, 64.7 ± 17.0 mL/min/1.73 m^2). The mean age of the potential kidney donors was less than in patients with aortic dissection (p = 0.00011) and patients with renovascular hypertension (p = 0.020).

Contrast flow in the renal artery on the MDCT angiography in the 90 subjects indicated normal flow in 66 (73.3%) subjects, of whom 44 were donors and 22 had aortic dissection (15, connected to a true lumen; seven, connected to a false lumen). Possibly disturbed flow was identified in the remaining 24 subjects (26.7%); the renal arterial lesion was unilateral in all. They included 13 patients with renal artery stenosis (five on the right side and seven on the left side) and renovascular hypertension (one on the left, the donor) and 11 patients with aortic dissection (three on the right and four on the left with a compressed orifice of the artery by a false lumen) [Fig. 2A], one on the right and three on the left with dissection involving the artery). Seven (two on the right and five on the left) of the 11 patients with aortic dissection and possibly disturbed flow had focal perfusional defects in the cortex via the segmentation technique (Figs. 2B and 2C).

Renal scanning GFR ranged from 9.1 to 63.6 mL/min (mean, 35.0 ± 10.7 mL/min) for the right kidney and 4.7–70.4 mL/min (mean, 34.5 ± 12.9 mL/min) for the left kidney. Renal perfusional cortex volumes in the first dataset from user 1 ranged from 52 to 195 mL (mean, 109.2 ± 27.0 mL) in the right kidney and 24–171 mL (mean, 104.5 ± 30.5 mL) in the left.

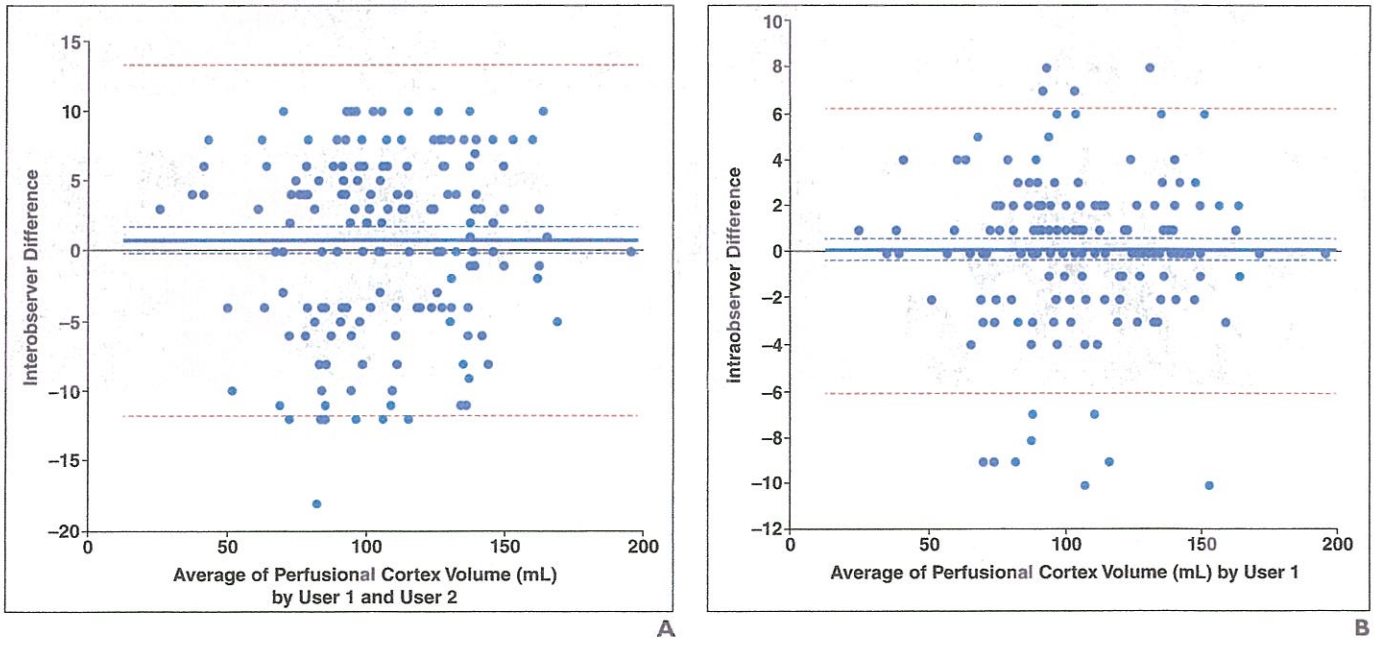

Fig. 3—Bland-Altman analyses. Solid line indicates bias, outer dotted lines indicate 95% CI, and inner dotted lines indicate 95% CI for bias.
A. Bland-Altman plot shows interobserver comparison of renal perfusional cortex volume measurements by two observers.
B. Bland-Altman plot for intraobserver comparison of renal perfusional cortex volume measurements.

TABLE 2: Univariate Correlations of Renal Perfusion Cortical Volume, Renal Parenchymal Volume, and Renal Glomerular Filtration Rate (GFR) With Age, Sex, Body Habitus, and Renal Function

Characteristic	Total Perfusional Cortical Volume (mL)	Total Parenchymal Volume (mL)	Total Renal Scanning GFR (mL/min)
Value (mean ± SD) [range]	213.0 ± 47.6 (114–352)	287.2 ± 56.3 (145–392)	73.8 ± 22.2 (23.4–132.6)
Univariate correlation			
Age	−0. 374 (0.0003)	−0.344 (0.0009)	−0.356 (0.0006)
Male/female ratio	0.235 (0.0263)	0.308 (0.0033)	−0.002 (NS)
Weight	0.418 (< 0.0001)	0.383 (0.0002)	0.0009 (NS)
BSA	0.400 (< 0.0001)	0.394 (0.0001)	−0.015 (NS)
Serum level of creatinine	−0.370 (0.0003)	−0.348 (0.0008)	−0.451 (< 0.0001)
eGFR by modified MDRD	0.558 (< 0.0001)	0.407 (< 0.0001)	0.611 (< 0.0001)
Potentially disturbed flow in the renal artery[a]	−0.323 (0.002)	−0.308 (0.0033)	−0.137 (NS)

Note—Except for value, numbers in parenthesis indicate *p* values. BSA = body surface area, eGFR = estimated glomerular filtration rate, MDRD = Modification of Diet in Renal Disease, NS = not statistically significant.
[a]Stenosis, dissection, or compression of the orifice by false lumen.

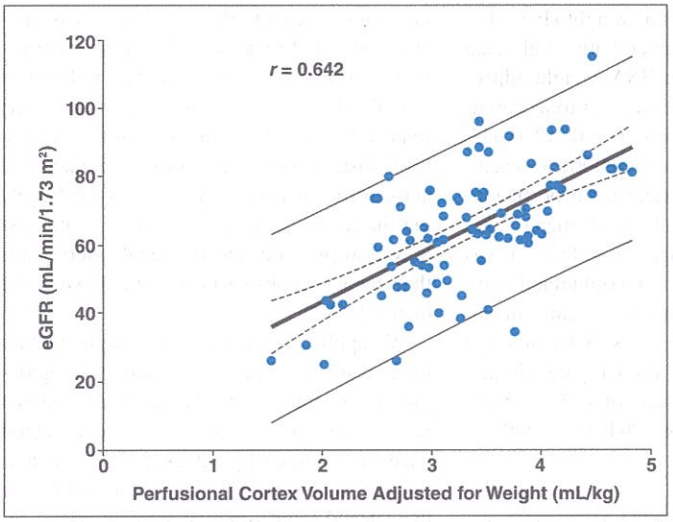

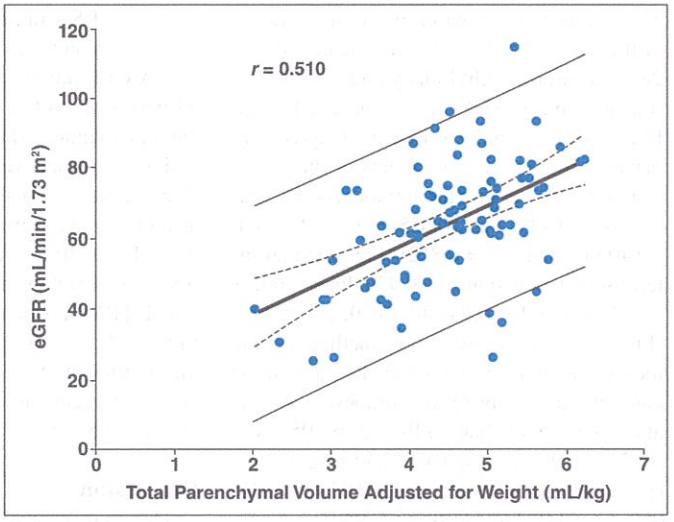

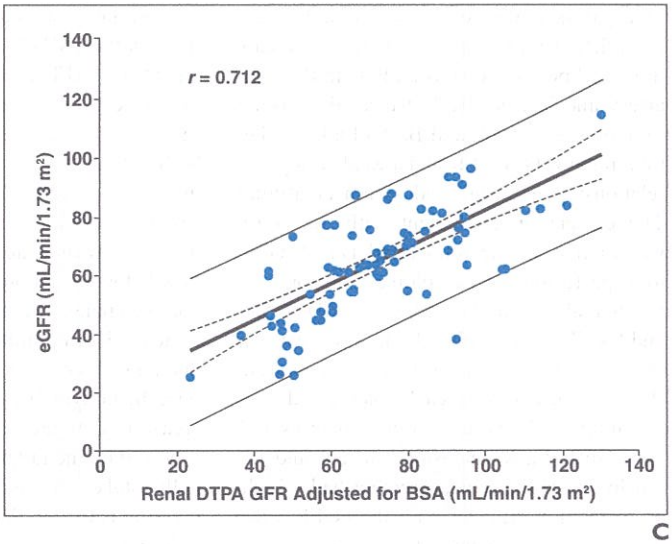

Fig. 4—Scatterplots with regression lines of renal volume measures and glomerular filtration rate (GFR) measured by renal diethylenetriamine pentaacetic acid (DTPA) scanning versus estimated GFR (eGFR) calculated with modified Modification of Diet in Renal Disease equation.
A, Scatterplot shows weight-adjusted total volume of renal perfusional cortex.
B, Scatterplot shows weight-adjusted total volume of renal parenchyma.
C, Scatterplot shows body surface area (BSA)–adjusted total GFR estimated by renal DTPA scanning using modified Gates method.

TABLE 3: Simple Linear Regression Analyses With Relationships of Each Renal Volume Measure Adjusted for Body Habitus Indexes and Renal Diethylenetriamine Pentaacetic Acid (DTPA) Scanning Glomerular Filtration Rate (GFR)

Adjusted	Total Renal Perfusional Cortical Volume (mL)	Total Renal Parenchymal Volume (mL)	Total Renal DTPA GFR (mL/min)
Weight			
r	0.642[a]	0.510[a]	0.505[a]
β	15.960	10.307	18.491
95% CI	11.92–19.99	6.625–13.99	11.80–25.18
BSA			
r	0.630[a]	0.482[a]	0.712[a]
β	0.440	0.276	0.631
95% CI	0.325–0.555	0.170–0.382	0.499–0.763

Note—BSA = body surface area, *r* = correlation coefficient, β = standardized regression coefficient.
[a] $p < 0.0001$.

The parenchymal volume in the first dataset of the user 1 was 63–197 mL (mean, 140.5 ± 28.3 mL) in the right kidney and 72–206 mL (mean, 146.2 ± 32.4 mL) in the left kidney. Bland-Altman analysis indicated agreement between the two measurements of the perfusional cortex volume for intraobserver variation ($r = 0.994$; bias, 0.055 ± 3.12; 95% CI, −0.403 to 0.513; $p = 0.812$) (Fig. 3A) and interobserver variation ($r = 0.976$; bias, 0.691 ± 6.397; 95% CI, −0.248 to 1.629; $p = 0.148$) (Fig. 3B). The segmentation method for the measurement of renal parenchyma volume had similar variability in intraobserver variation ($r = 0.994$; bias, 0.10 ± 3.08; 95% CI, −0.372 to 0.572; $p = 0.676$) and interobserver variation ($r = 0.974$; bias, −0.033 ± 7.028; 95% CI, −1.067 to 1.000; $p = 0.949$).

Each total perfusional cortex volume and total parenchymal volume had weakly negative relationships to age, serum level of creatinine, and possibly disturbed flow in the renal artery and had positively weak relationships to male sex, weight, and BSA (Table 2). The total renal DTPA GFR had a weakly negative relationship with age and serum creatinine. The correlation coefficient with the eGFR was higher for the total renal DTPA GFR, total perfusion cortex volume, and total parenchymal volume in rank ($r = 0.611$, 0.558, and 0.407, respectively). Table 3 presents the results of simple linear regression analysis showing correlation of each volume and renal scanning GFR adjusted for body habitus with the eGFR. Each perfusion cortical and parenchymal volume measurement had a higher correlation efficient with the eGFR when the volume was adjusted for weight rather than BSA (Figs. 4A and 4B). Renal DTPA scanning GFR had a higher correlation coefficient with the eGFR when the GFR was adjusted for BSA rather than weight (Fig. 4C). The coefficient was higher with total renal DTPA GFR adjusted for BSA, weight-adjusted perfusion cortex volume, and total parenchymal volume in that order ($r = 0.712$, 0.642, and 0.510, respectively) ($p < 0.0001$ for each). The coefficient for the right renal perfusional cortex volume percent with a mean value of 52.1% ± 10.1% (range, 26.4–89.5%) was 0.826 ($p < 0.0001$) and for the right renal scanning DTPA GFR percent with a mean value of 51.0% ± 12.1% (range, 22.0–89.5%), although the coefficient of the right renal parenchymal volume percent with a mean of 49.5% ± 5.5% (range, 36.5–79.7%) was 0.764 ($p < 0.0001$).

Discussion

This study showed that the perfusional cortex volume adjusted for weight had a moderate correlation with the eGFR calculated with the modified MDRD equation, similar to renal DTPA GFR adjusted for BSA. The adjusted perfusional cortex volume, for which the correlation coefficient with the eGFR was higher than the adjusted parenchymal volume, was revealed to be more useful in assessing renal function. Whole-kidney volume decreases with acute reduction in renal blood flow below the autoregulatory range, with the volume change presumed to be mainly in the cortex [13]. In animal models, with acute reductions of renal blood flow, the earliest intrarenal hemodynamic change observed is a decrease in the outer cortical renal blood flow, followed by medullary hypoperfusion, and finally total cortical ischemia as renal perfusion pressure is further decreased [13].

Renal artery disease may lead to both hypertension and deterioration in renal function. Both of these processes likely develop with accompanying disturbances in renal blood flow, either to the whole kidney or specific intrarenal regions as shown in some patients with aortic dissection. The bulging of the false lumen can produce occlusion at the renal arterial orifice, and subsequent thrombosis distally may occur. Intimal detachment at the orifice may occur with perfusion largely via the false channel. The dissection process may also proceed into the renal artery, such that the actual obstruction occurs beyond the orifice [13].

We applied a semiautomatic segmentation method for liver analysis driven by a region-growing technique based on the postulate that neighboring pixels within the same region have similar intensity values [14]. The region-growing technique provides a useful ROI for the arterial input function semiautomatic selection of ROI in which the neighboring pixels within the same region have similar attenuation. This study showed that operators might have very little influence on the accuracy of manual editing for interactive cutting of the vessels with the software. In previous studies of normal kidneys, the cortical volume adjusted for body habitus has been reported to have similar correlation coefficients to the parenchymal volume as renal function [5, 9], but the perfusional cortex volume measurement for potential donors, patients with renovascular hypertension, and patients with aortic dissection could be shown to be superior to the parenchymal volume measurement for renal function in this study. The 5–10 minutes required for the perfusional cortex volume measurement for each kidney are acceptable in clinical use.

The measured clearance of nonionic contrast agent in a dynamic CT dataset using Patlak plot analysis has been reported to have a strong correlation with the total GFR

calculated by urinary creatinine clearance and is superior to renal DTPA GFR [15]. The volume measurement by the semiautomatic segmentation technique we used in this study has an advantage in terms of radiation exposure and cost because the measurement can be performed using volumetric data for MDCT angiography for evaluation of renal vascular anatomy and disease.

Radiation exposure due to MDCT has raised concern in young donors and patients with renovascular hypertension. Single-phase MDCT angiography performed on a 16-MDCT scanner has been suggested to be associated with an approximately 20-mSv radiation dose, whereas MDCT systems with more than 64-MDCT and with wider-area detector scanners enable lower radiation doses because of their shorter scanning times and the reduction of redundant radiation from overlapping of sequential axial scanning. Recently, advances in iterative reconstruction and automated exposure control have achieved a 20–30% reduction in radiation exposure [16].

In this study of Japanese subjects, the correlation coefficient of the renal DTPA GFR with eGFR calculated by the modified MDRD equation was limited to 0.712, which is considered moderate correlation. Because it uses inulin clearance as the reference standard, the Gates method tends to overestimate GFR at low levels and underestimate GFR at high levels [17]. DTPA is not a GFR substance, and 5–10% of the ^{99m}Tc-DTPA is plasma protein–bounded, resulting in underestimation of true GFR by approximately 10%. The technique also has a limitation in that the measurement by a parallel-hole gamma camera is affected by the selection of the ROI for each kidney and the kidney depth [18]. In contrast to renal DTPA scanning, CT angiography before the era of MDCT provided no data regarding renal perfusion or function [19]. However, this study shows that renal perfusion cortex volume measured by volumetric data for MDCT angiography may replace renal DTPA scanning. Replacing renal DTPA scanning with renal perfusion cortex volume may be limited to subjects who require renal MDCT angiography, such as potential kidney donors and patients with renovascular disease and aortic dissection. Serial follow-up studies using perfusion cortical volume measurement are not recommended in patients with impaired renal function because of nephrotoxicity of contrast material. Follow-up study is also not recommended in young patients with renal arterial stenosis because of radiation exposure.

There are some limitations to this study. First, in this retrospective study, which included quantitative evaluation of the measurements, the observer may have affected the measurements of the MDCT images. Second, inulin clearance, which is an ideal method for determining GFR, was not obtained. Third, the renal DTPA scanning we performed in this study was not the original method using venous sampling but rather the modified Gates method.

In conclusion, weight-adjusted renal perfusional cortical volume measured using MDCT renal angiography with 5-mm collimation had a higher correlation with eGFR than did parenchymal volume. Therefore, renal perfusional cortical volume may be used to provide renal functional information as well as renal DTPA scanning using the modified Gates method.

References

1. Gates GF. Split renal function testing using Tc-99m DTPA: a rapid technique for determining differential glomerular filtration. *Clin Nucl Med* 1983; 8:400–407
2. Shokeir AA, el-Diasty TA, Nabeeh A, et al. Digital subtraction angiography in potential live-kidney donors: a study of 1000 cases. *Abdom Imaging* 1994; 19:461–465
3. Aburano T, Yokoyama K, Taki J, et al. Asymmetric abnormality of renal perfusion with symmetric function in aortic dissection. *Clin Nucl Med* 1992; 17:36–40
4. Chen X, Summers RM, Cho M, Bagci U, Yao J. An automatic method for renal cortex segmentation on CT images: evaluation on kidney donors. *Acad Radiol* 2012; 19:562–570
5. Muto NS, Kamishima T, Harris AA, et al. Renal cortical volume measured using automatic contouring software for computed tomography and its relationship with BMI, age and renal function. *Eur J Radiol* 2011; 78:151–156
6. Mazonakis M, Damilakis J, Varveris H, Prassopoulos P, Gourtsoyiannis N. Image segmentation in treatment planning for prostate cancer using the region growing technique. *Br J Radiol* 2001; 74:243–248
7. Saxena AB, Busque S, Arjane P, Myers BD, Tan JC. Preoperative renal volumes as a predictor of graft function in living donor transplantation. *Am J Kidney Dis* 2004; 44:877–885
8. Li X, Chen X, Yao J, Zhang X, Yang F, Tian J. Automatic renal cortex segmentation using implicit shape registration and novel multiple surfaces graph search. *IEEE Trans Med Imaging* 2012; 31:1849–1860
9. Yano M, Lin MF, Hoffman KA, Vijayan A, Pilgram TK, Narra VR. Renal measurements on CT angiograms: correlation with graft function at living donor renal transplantation. *Radiology* 2012; 265:151–157
10. Helck A, Wessely M, Notohamiprodjo M, et al. CT perfusion technique for assessment of early kidney allograft dysfunction: preliminary results. *Eur Radiol* 2013; 23:2475–2481
11. Imai E, Horio M, Nitta K, et al. Estimation of glomerular filtration rate by the MDRD study equation modified for Japanese patients with chronic kidney disease. *Clin Exp Nephrol* 2007; 11:41–50
12. Zou KH, Tuncali K, Silverman SG. Correlation and simple linear regression. *Radiology* 2003; 227:617–622
13. Mattson DL, Lu S, Roman RJ, Cowley AW Jr. Relationship between renal perfusion pressure and blood flow in different regions of the kidney. *Am J Physiol* 1993; 264(3 Pt 2):R578–R583
14. Lu Y, Jiang T, Zang Y. Region growing method for the analysis of functional MRI data. *Neuroimage* 2003; 20:455–465
15. Tsushima Y, Blomley MJ, Okabe K, Tsuchiya K, Aoki J, Endo K. Determination of glomerular filtration rate per unit renal volume using computerized tomography: correlation with conventional measures of total and divided renal function. *J Urol* 2001; 165:382–385
16. Chen MY, Shanbhag SM, Arai AE. Submillisievert median radiation dose for coronary angiography with a second-generation 320-detector row CT scanner in 107 consecutive patients. *Radiology* 2013; 267:76–85
17. De Santo NG, Anastasio P, Cirillo M, et al. Measurement of glomerular filtration rate by the ^{99m}Tc-DTPA renogram is less precise than measured and predicted creatinine clearance. *Nephron* 1999; 81:136–140
18. O'Reilly PH, Pollard AJ. Nephroptosis: a cause of renal pain and a potential cause of inaccurate split renal function determination. *Br J Urol* 1988; 61:284–288
19. Pedersen EB. New tools in diagnosing renal artery stenosis. *Kidney Int* 2000; 57:2657–2677